Shen *et al. IMA Fungus* (2023) 14:11
https://doi.org/10.1186/s43008-023-00116-7

IMA Fungus

RESEARCH

Open Access

Taxonomy of *Hyphodermella*: a case study to show that simple phylogenies cannot always accurately place species in appropriate genera

Shan Shen[1,2†], Shi-Liang Liu[1†] and Li-Wei Zhou[1*]

Abstract

The genus is a special and crucial taxonomic rank compared with others above the species level, because a species has to be placed in a certain genus instead of any other higher ranks. With more and more new species being described, the placements of their generic position are sometimes incorrect due to the simple phylogenies resulting from inappropriate sampling. Here, we focus on the taxonomy of a small wood-inhabiting fungal genus *Hyphodermella*. With the most comprehensive sampling to date, the phylogenetic position of *Hyphodermella* within *Phanerochaetaceae* is rearranged by employing the same ITS and nLSU regions as in previous studies and also the ITS, nLSU, *rpb1*, *rpb2* and *tef1a* regions. Three species are excluded from *Hyphodermella*: *H. poroides* is placed in a newly introduced monotypic genus *Pseudohyphodermella*, while *H. aurantiaca* and *H. zixishanensis* are transferred to *Roseograndinia*. *Hyphodermella suiae* is described as a new species from South China and Vietnam. Keys to eight species in *Hyphodermella* and five in *Roseograndinia* are provided. Beyond solving the taxonomic issue of *Hyphodermella* itself, the current study also aims to suggest that all fungal taxonomists especially beginners should keep in mind to sample as many comprehensive taxa as possible in phylogenetic analyses.

Keywords Wood-inhabiting fungi, *Basidiomycota*, *Phanerochaetaceae*, *Pseudohyphodermella*, *Roseograndinia*, Five new taxa

INTRODUCTION

Despite being one of the most species-rich life forms, *Fungi* are poorly documented with more than 90% of estimated species (2.2 to 3.8 million species) awaiting formal description (Hawksworth and Lücking 2017). To enlarge the knowledge of fungal diversity, more than one thousand species have been newly introduced each year during the last decades (Dai et al. 2015; Hawksworth and Lücking 2017; Niskanen et al. 2018). Above the species level, genus is a special and crucial taxonomic rank compared with other ranks under the binomial nomenclature system, because a species has to be placed in a certain genus but may be not assigned in any certain higher rank than genus. Although molecular phylogenies are helpful to determine the generic position of fungal species, the placements are sometimes incorrect due to the use of simple phylogenies resulted from inappropriate sampling in a bad practice of phylogenetic analyses. Here, a simple phylogeny is defined to sample only targeted species but not closely related outgroup taxa; in this way, the generic circumscription cannot be reliably delimited (Fig. 1). In contrast, a "good" genus can only be accurately delimited by sampling

†Shan Shen and Shi-Liang Liu have contributed equally to this work.

*Correspondence:
Li-Wei Zhou
liwei_zhou1982@im.ac.cn
[1] State Key Laboratory of Mycology, Institute of Microbiology, Chinese Academy of Sciences, Beijing 100101, People's Republic of China
[2] University of Chinese Academy of Sciences, Beijing 100049, People's Republic of China

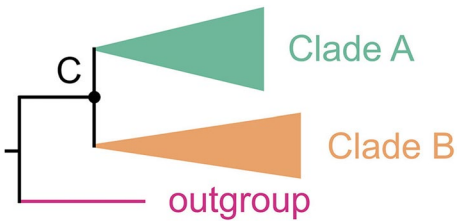

Fig. 1 A schematic illustration of the 'simple phylogeny' resulted from inappropriate sampling in a bad practice of phylogenetic analyses. Whatever the statistical support at the node C is high or not, species in Clade A is not always congeneric with species in Clade B

more related taxa to the targeted species. Indeed, increased taxon sampling has long been known as an efficient method to reduce error signals in phylogenetic analyses (Zwickl and Hillis 2002; Prasanna et al. 2020).

To clearly present the results of simple phylogenetic studies in fungal taxonomy and the resulting incorrect generic placements of taxa, two examples recently dealt with by us are briefly summarized here. One is the incorrect placements at the generic level of two species originally placed in *Heteroradulum*, viz. *H. yunnanense* (with the wrong masculine gender as '*yunnanensis*'; Guan et al. 2020) and *H. niveum* (Li et al. 2022a). In Guan et al. (2020), several taxa of *Heteroradulum* were selected as the only ingroup and *H. yunnanense* was placed at the basal position within the so-called *Heteroradulum* lineage; actually, this simple phylogeny cannot determine whether *H. yunnanense* should be the member of *Heteroradulum* or not. With the help of a more comprehensive sampling, a later phylogenetic analysis clearly separated *H. yunnanense* from *Heteroradulum* and thus excluded it from this genus (Li et al. 2022b).

Similarly, according to a simple phylogeny (Li et al. 2022a: Fig. 2) adopted from Guan et al. (2020), the new species *Heteroradulum niveum* was further incorrectly placed in *Heteroradulum* (Li et al. 2022a). Even worse, the accompanying phylogeny in that paper (Li et al. 2022a: Fig. 1) did not cluster *H. niveum* with other species of *Heteroradulum* with reliable statistical support at all. In contrast, Liu et al. (2022b) thoroughly explored the phylogenetic relationships among *Heteroradulum* and its close genera, which resulted in a new genus *Alloexidiopsis* for the clade composed of *H. yunnanense* and *H. niveum*.

Another example is two species originally placed in *Trechispora* (Zong et al. 2021) and then in *Brevicellicium* (Liu et al. 2022c). In Zong et al. (2021), newly describing *Trechispora daweishanensis* and *T. xantha*, the first phylogeny did not recover the monophyly of *Trechispora* with these two species, while the second one simply including taxa only from *Trechispora* as the ingroup clustered the two species with *T. yunnanensis* and separated them from additional species of *Trechispora*. As first noted by Chikowski et al. (2020) and then confirmed by Liu et al. (2022a), the ITS and nLSU sequences from specimens of *T. yunnanensis* (Xu et al. 2019) actually represent different species from *Trechisporales* and *Hymenochaetales*, respectively, and thus the phylogenetic position of *T. yunnanensis* itself is doubtful. Liu et al. (2022c) recognized the incorrect generic placements of *T. daweishanensis* and *T. xantha* by Zong et al. (2021), and transferred these two species to *Brevicellicium*. However, the phylogeny supporting these transfers was also on the basis of a simple phylogeny (Liu et al. 2022c: Fig. 1), in which these two species also clustered together with species of *Brevicellicium* but occupied a separated position. By sampling the most comprehensive range of taxa in *Trechisporales* available to date, the phylogeny in Liu et al. (2022a) clarified these two species placing them outside of both *Trechispora* and *Brevicellicium*, and in a new genus, *Allotrechispora*.

Besides the examples of *Heteroradulum*, *Trechispora*, and *Brevicellicium* having been dealt with (Li et al. 2022b; Liu et al. 2022a, b), similar incorrect placements also exist in other genera. In the current study, we focus on the genus *Hyphodermella*, in which two recently collected specimens from tropical Asia are identified.

Hyphodermella was erected as a monotypic genus for *H. corrugata* (Eriksson and Ryvarden 1976). Besides the generic type, another eight species are accepted in this genus within *Phanerochaetaceae* (Gilbertson et al. 2001; Melo and Hjortstam 2003; Nakasone 2008; Duhem 2010; Telleria et al. 2010; Duhem and Buyck 2011; Zhao et al. 2017; Wang and Zhao 2020; Wang et al. 2021a). Within *Hyphodermella*, the generic placement of *H. poroides* is questionable. *Hyphodermella poroides* was described according to a simple phylogeny that placed this species in a basal position within a clade also comprising *H. corrugata* and *H. rosae* (Zhao et al. 2017). Besides the uncertain phylogenetic position, the poroid hymenophoral surface also makes *H. poroides* distinguished from other species of *Hyphodermella* (Zhao et al. 2017). Although macrofungal species producing various hymenophoral configurations commonly can be placed in the same genus (Wang et al. 2021b; Li et al. 2022b; Liu et al. 2022a), in this case it is obvious, not as stated in the Abstract by the authors: "Both morphological and molecular evidences confirmed the placement of the new species in *Hyphodermella*." (Zhao et al. 2017). Chen et al. (2021) recently performed a much more comprehensive phylogenetic analysis than that of Zhao et al. (2017) which clearly revealed the separation of *H. poroides* from

Hyphodermella (Chen et al. 2021: Fig. 3), but they did not make any taxonomic change possibly due to their focusing mainly on other taxonomic issues. Around the publication time of Chen et al. (2021), another two new species, viz. *H. aurantiaca* and *H. zixishanensis* were separately described in *Hyphodermella* by the same research group, although the related phylogenies never confirmed their close relationship with *Hyphodermella* (Wang and Zhao 2020; Wang et al. 2021a).

When examining our specimens of *Hyphodermella*, we also explored the phylogenetic relationship of this genus via the most comprehensive sampling available to date. Accordingly, one genus, one species and three combinations are newly proposed. Beyond the taxonomic issue of *Hyphodermella*, we also aim to provide a standard to better phylogenies in future taxonomic studies.

MATERIALS and METHODS

Morphological examination

The studied specimens are preserved at the Fungarium, Institute of Microbiology, Chinese Academy of Sciences (HMAS), Beijing, China. The hymenophoral surfaces of basidiomes were examined with a Leica M125 stereomicroscope (Wetzlar, Germany) at a magnification of up to 100×. The microscopic characters were observed with an Olympus BX43 light microscope (Tokyo, Japan) at magnifications up to 1000×. The microscopic procedure followed Yu et al. (2021). Basidiome sections were prepared with Cotton Blue (CB), Melzer's reagent, and 5% potassium hydroxide (KOH). All measurements were made from sections in CB. When presenting the variation of basidiospore sizes, 5% of the measurements were excluded from each end of the range and are given in parentheses. Drawings were made with the aid of a drawing tube. In the morphological description, L = mean basidiospore length (arithmetic average of all measured basidiospores), W = mean basidiospore width (arithmetic average of all measured basidiospores), Q = variation in the L/W ratios between the studied specimens, and (a/b) = the number of measurements (a) from a given number (b) of specimens.

Molecular sequencing

A small piece of basidiome was taken for DNA extraction using a CTAB rapid plant genome extraction kit-DN14 (Aidlab Biotechnologies, Beijing). Then, the crude DNA was used as templates for PCR amplifications of ITS, nLSU, *rpb1*, *rpb2* and *tef1α* regions with the primer pairs ITS5/ITS4 (White et al. 1990), LROR/LR7 (Gardes and Bruns 1993), RPB1-Af/RPB1-Cr (Matheny et al. 2002), RPB2-f5F/RPB2-b7.1R (Liu et al. 1999; Matheny 2005) and 983F/1567R (Rehner and Buckley 2005), respectively. The PCR procedure was as follows: initial denaturation at 95 °C for 3 min, followed by 34 cycles at 94 °C for 40 s, 57.2 °C for 45 s and 72 °C for 1 min, and a final extension at 72 °C for 10 min for ITS and *tef1α* regions; initial denaturation at 94 °C for 1 min, followed by 35 cycles at 94 °C for 30 s, 48 °C 1 min and 72 °C for 1.5 min, and a final extension of 72 °C for 10 min for nLSU region; initial denaturation at 94 °C for 2 min, followed by 10 cycles at 94 °C for 45 s, 60 °C for 45 s (minus 1 °C per cycle) and 72 °C for 1.5 min, then followed by 36 cycles at 94 °C for 45 s, 53 °C for 1 min and 72 °C for 1.5 min, and a final extension of 72 °C for 10 min for *rpb1* and *rpb2* regions. The PCR products were sequenced with the same primers as those used in PCR amplification at the Beijing Genomics Institute, Beijing, China. All newly generated sequences were deposited in GenBank (https://www.ncbi.nlm.nih.gov/genbank/; Table 1).

Phylogenetic analyses

Besides the newly generated sequences, additional molecular sequences were downloaded from GenBank for the phylogenetic analysis (Table 1). Two datasets were assembled to explore the phylogenetic position of our specimens in *Hyphodermella* and, more importantly, the phylogenetic relationship among *Hyphodermella* and related genera within *Phanerochaetaceae*. For the dataset of the combined ITS and nLSU regions, genera represented mostly by generic types in *Phanerochaetaceae* as well as *Irpicaceae* and *Meruliaceae* were comprehensively sampled as ingroup taxa. *Hyphoderma litschaueri*, *H. mutatum* and *Candelabrochaete africana* were selected as outgroup taxa (Chen et al. 2021). For the dataset of combined ITS, nLSU, *rpb1*, *rpb2* and *tef1α* regions, genera phylogenetically close to our specimens were further sampled as ingroup taxa and *Gelatinofungus brunneus* was selected as the outgroup taxon according to the topology resulting from the previous two-locus dataset. ITS, nLSU, *rpb1*, *rpb2* and *tef1α* regions were separately aligned using MAFFT 7.110 (Katoh and Standley 2013) under the G-INS-i option (Katoh et al. 2005), and the ambiguous regions of the alignments were trimmed using trimAl v1.2 under default parameters (Capella-Gutiérrez et al. 2009). Firstly, the resulting alignments for each locus were separately subjected to phylogenetic analyses, and no conflict in main lineages of our targeted taxonomic groups was observed from each other (data not shown). Then, the resulting alignments were concatenated as two alignments corresponding to the two datasets (Additional file 1: Alignment S1, Additional file 2: Alignment S2). The ITS region in these two alignments were further divided into ITS1, 5.8S and ITS2 subregions using ITSx 1.1.2 (Bengtsson-Palme et al. 2013) for separate model selection of phylogenetic analyses.

The maximum likelihood (ML) algorithm was performed using IQ-tree v2.1.2 (Minh et al. 2020), which implements automatic substitution model selection for each locus in ModelFinder (Kalyaanamoorthy et al. 2017) assessing nodal support determined by ultrafast bootstrapping (BS) with 10,000 replicates. The Bayesian inference (BI) algorithm was performed using MrBayes 3.2 (Ronquist et al. 2012). jModelTest 2 was used to estimate the best-fit evolutionary models of all loci separately for the BI algorithm under the corrected Akaike information criterion (Guindon and Gascuel 2003; Posada 2008). A discrete gamma distribution was used to model evolutionary rate differences among sites (four categories, +G). In the BI algorithm, two independent runs, each with four chains of one million generations and starting from random trees, were employed; trees were sampled every 1000th generation, of which the first 25% were removed as burn-in and the other 75% were retained for constructing a 50% majority consensus tree and calculating Bayesian posterior probabilities (BPPs). Tracer 1.5 (http://tree.bio.ed.ac.uk/software/tracer/) was used to judge whether chains converged.

RESULTS

Seven new sequences were generated from our specimens for this study (Table 1). The concatenated alignment of ITS and nLSU regions included 1643 characters with 311 parsimony-informative ones from 87 collections representing 68 species. For the ML algorithm, the best-fit partitioned models were determined as TVM+F+I+I+R4 for ITS1, GTR+F+I+I+R3 for both 5.8S and nLSU, and GTR+F+R4 for ITS2. For the BI algorithm, K80+G, JC, JC and GTR+I+G were estimated as the best-fit partitioned models for the partitions of ITS1, 5.8S, ITS2 and nLSU, respectively. All chains in BI converged after ten million generations, which is indicated by the effective sample sizes of all parameters above 200 and the potential scale reduction factors close to 1.000. ML and BI algorithms construct similar topologies that differed only at several poorly supported nodes. The topology resulted from the ML algorithm is shown along with BS values more than 50% and BPPs more than 0.8 at the nodes (Fig. 2). In this phylogeny, the sampled species of *Hyphodermella* are separated in three lineages within the *Donkia* clade of *Phanerochaetaceae* (Fig. 2). The core lineage comprises the generic type *Hyphodermella corrugata*, *H. pallidostraminea* and *H. rosae* (BS=92%, BPP=0.99). In addition, two newly sequenced specimens, viz. LWZ 20190613-54 from Guangdong, China and LWZ 20191208-13 from Malaysia fall within the core lineage of *Hyphodermella*, and are separated from other species in this lineage. *Hyphodermella aurantiaca* and *H. zixishanensis* grouped together with two species of *Roseograndinia* (BS=99%, BPP=0.95). *Hyphodermella poroides* forms an independent lineage from other genera and species (BS=100%, BPP=1).

The concatenated alignment of ITS, nLSU, *rpb1*, *rpb2* and *tef1α* regions included 4550 characters with 882 parsimony-informative ones from 22 collections representing 18 species. For the ML algorithm, the best-fit partitioned models were determined as TPM2u+F+I+I+R2 for ITS1, TN+F+R2 for both 5.8S and nLSU, TIM+F+I+I+R2 for ITS2, GTR+F+I+I+R3 for both *rpb1* and *rpb2*, and TIM2+F+I+I+R2 for *tef1α*. For the BI algorithm, SYM+G, K80 and HKY+I+G were estimated as the best-fit partitioned models for the partitions of ITS1, 5.8S and ITS2, respectively, and GTR+I+G for all of nLSU, *rpb1*, *rpb2* and *tef1α*. All chains in BI converged after one million generations, which is indicated by the effective sample sizes of all parameters above 200 and the potential scale reduction factors close to 1.000. ML and BI algorithms construct similar topologies that differed only at several poorly supported nodes. The topology resulted from the ML algorithm is shown along with BS values more than 50% and BPPs more than 0.8 at the nodes (Fig. 3). Like the phylogeny inferred from the dataset of combined ITS and nLSU regions (Fig. 2), this five-locus based phylogeny also recovered the sampled species of *Hyphodermella* in three independent lineages and the distinct position of the two newly sequenced specimens within the core lineage (Fig. 3).

In association with morphological characters, the two newly sequenced specimens are described as a new species of *Hyphodermella*, a new genus is erected for *H. poroides*, and *H. aurantiaca* and *H. zixishanensis* are transferred to *Roseograndinia*.

TAXONOMY

Hyphodermella suiae Shan Shen, S.L. Liu & L.W. Zhou, **sp. nov.** (Figs. 4, 5)

MycoBank: MB 848641

Etymology: *suiae* (Lat.), in memory of the Chinese mycologist Hong-Yan Su (苏 鸿雁), who was a professor in Dali University and kindly helped the corresponding author in many ways; she passed away on 3 May 2022 during the preparation of the current paper at the age of 55 years.

Diagnosis: Distinguished from other species of *Hyphodermella* by the small basidiospores.

Type: **China:** *Guangdong*: Ruyuan County, Nanling National Forest Park, on fallen angiosperm twig, 13

Table 1 Species and sequences used in phylogenetic analyses

Species name	Collection No	Collection locality	Collection date	Accession No				
				ITS	nLSU	*rpb1*	*rpb2*	*tef1α*
Alboefibula bambusicola	Chen 2304	China: Taiwan	27 Jun 2014	MZ636926	MZ637091	MZ748355	OK135980	MZ913590
Alboefibula bambusicola	Wu 1209-26	China: Taiwan	15 Sept 2012	MZ636927	MZ637092			
Alboefibula gracilis	Wu 1809-106	China: Guangxi	10 Sept 2018	MZ636929	MZ637094	MZ748357	OK135982	MZ913591
Alboefibula gracilis	Wu 1809-152	China: Guangxi	10 Sept 2018	MZ636930	MZ637095			
Bjerkandera adusta	HHB-12826-Sp	USA: Alaska		KP134983	KP135198			
Byssomerulius corium	FP-102382	USA: Wisconsin		KP135007	KP135230			
Candelabrochaete africana	FP-102987-Sp	USA: Puerto Rico		KP135294	KP135199			
Ceriporia purpurea	KKN 223	USA: Arizona		KP135044	KP135203			
Ceriporia viridans	GC 1708-211	China: Yunnan		LC427027	LC427049			
Climacodon septentrionalis	AFTOL-767	Unknown		AY854082	AY684165			
Crepatura ellipsospora	CLZhao 1260	China: Yunnan	22 Apr 2017	MK343693	MK343697			
Crepatura ellipsospora	CLZhao 1265	China: Yunnan	22 Apr 2017	MK343692	MK343696			
Crystallicutis damiettensis	UN63	Egypt: Kafr El-Sheikh, Baltim	14 Feb 2014	MW508515	MW508515			
Crystallicutis serpens	HHB-15692-Sp	USA: Alaska		KP135031	KP135200			
Donkia pulcherrima	GC 1707-11	China: Taiwan	23 Jul 2017	LC378994	LC379152	LC379157	LC387351	LC387371
Donkia pulcherrima	Gothenburg-2022	Austria		KX752591	KX752591			
Efibulella deflectens	FCUG 1568	Sweden		AF141619	AF141619			
Emmia latemarginata	CBS 436.48	Canada: British Columbia		MH856427	MH867973			
Gelatinofungus brunneus	Wu 1207-162	China: Taiwan	10 Jul 2012	MZ636978	MZ637139	MZ748366	OK136005	MZ913615
Gelatinofungus brunneus	Wu 1207-163	China: Taiwan	10 Jul 2012	MZ636979	MZ637140			
Geliporus exilisporus	Dai 2172	China: Liaoning	25 Sept 1995	KU598211	KU598216			
Geliporus exilisporus	GC 1702-15	China: Taiwan	19 Feb 2017	LC378995	LC379153	LC379158	LC387352	LC387372
Gloeoporus conchoides	BZ-2896	Belize		MG572757	MG572741			
Gloeoporus pannocinctus	L-15726-Sp	USA: New York		KP135060	KP135214			
Hapalopilus eupatorii	Dammrich 10744	Germany		KX752620	KX752620			
Hapalopilus percoctus	H 7008581	Botswana		KX752597	KX752597			
Hapalopilus rutilans	CBS 422.48	Canada: Ontario		MH856419	MH867966			
Hydnophlebia chrysorhiza	FD-282	USA: Florida		KP135338	KP135217			
Hyphoderma litschaueri	FP-101740-Sp	USA: Wisconsin		KP135295	KP135219			
Hyphoderma mutatum	HHB-15479-Sp	USA: Alaska		KP135296	KP135221			
Hyphodermella corrugata	MA-Fungi 24238	Portugal	28 Apr 1989	FN600378	JN939586			
Hyphodermella corrugata	MA-Fungi 5527	Morocco	20 Jun 1982	FN600372	JN939597			
Hyphodermella corrugata	MA-Fungi 61395	France	31 Oct 1998	FN600380	JN939584			
Hyphodermella pallidostraminea	LE 286968	Russia: Jewish Autonomous Oblast	24 Aug 2009	OK138912	OK138911			

Table 1 (continued)

Species name	Collection No	Collection locality	Collection date	Accession No				
				ITS	nLSU	*rpb1*	*rpb2*	*tef1a*
Hyphodermella rosae	FP-150552	USA: Hawaii		KP134978	KP135223			
Hyphodermella rosae	GC 1608-2	Japan		MZ636987	MZ637148	MZ748411	OK135983	MZ913592
Hyphodermella suiae	LWZ 20190613-54	China: Guangdong	13 Jun 2019	**ON614149**	**ON614151**	**OP698136**	**OP698133**	
Hyphodermella suiae	LWZ 20191208-13	Malaysia: Kuala Lumpur	08 Dec 2019	**ON614150**			**OP698134**	**OP698135**
Irpex lacteus	FD-9	USA: Massachusetts		KP135026	KP135224			
Meruliopsis albostramineus	HHB-10729	USA: Virginia		KP135051	KP135229			
Mycoacia fuscoatra	HHB-10782-Sp	USA: Wisconsin		KP135365	KP135265			
Odontoefibula orientalis	Wu 0805-59	China: Taiwan	22 May 2008	LC363488	LC363493			
Odontoefibula orientalis	Wu 0910-57	China: Beijing	14 Oct 2009	LC363490	LC363495	LC363501	LC387362	LC387381
Oxychaete cervinogilva	Dmitry Schigel 5216	Australia		KX752596	KX752596			
Phaeophlebiopsis caribbeana	HHB-6990	USA: Florida		KP135415	KP135243			
Phaeophlebiopsis peniophoroides	FP-150577	USA: Hawaii		KP135417	KP135273			
Phanerina mellea	Dai 9667	China: Hainan	26 May 2008	JX623933	JX644058			
Phanerina mellea	WEI 17-224	China: Taiwan	11 Jun 2017	LC387333	LC387340			
Phanerochaete alnea	Spirin 8829a	Canada: Alberta		KX538925				
Phanerochaete australis	HHB-7105-Sp	USA: Florida		KP135081	KP135240			
Phanerochaete burtii	HHB-4618-Sp	USA: Florida		KP135117	KP135241			
Phanerochaete canobrunnea	CHWC 1506-66	China: Taiwan	23 Jun 2015	LC412095	LC412104			
Phanerochaete ericina	HHB-2288	USA: North Carolina		KP135167	KP135247			
Phanerochaete fusca	Wu 1409-161	China: Hubei	19 Sept 2014	LC412098	LC412105			
Phanerochaete laevis	HHB-15519-Sp	USA: Alaska		KP135149	KP135249			
Phanerochaete porostereoides	He 1908	China: Shannxi	11 Sept 2013	KX212218	KX212222			
Phanerochaete pseudomagnoliae	PP-25	South Africa		KP135091	KP135250			
Phanerochaete rhodella	FD-18	USA: Massachusetts		KP135187	KP135258			
Phanerodontia chrysosporium	HHB-6251-Sp	USA: Arizona		KP135094	KP135246			
Phlebia centrifuga	HHB-9239-Sp	USA: Michigan		KP135380	KP135262			
Phlebia radiata	AFTOL-484	Unknown		AY854087	AF287885			
Phlebiopsis crassa	KKN-86-Sp	USA: Arizona		KP135394	KP135215			
Phlebiopsis flavidoalba	FD-263	USA: Florida		KP135402	KP135271			
Phlebiopsis gigantea	FP-70857-Sp	USA: Georgia		KP135390	KP135272			
Phlebiopsis pilatii	Spirin 5048	Russia		KX752590	KX752590			
Pirex concentricus	Kropp160Bup6-R	USA: Oregon		KP134985				
Pirex concentricus	OSC-41587	USA: Oregon		KP134984	KP135275	KP134843	KP134940	
Porostereum spadiceum	Wu 9708-104	China			DQ679918			
Pseudohyphodermella poroides	Dai 10848	China:Hainan	11 May 2009	KX008368	KX011853			

Table 1 (continued)

Species name	Collection No	Collection locality	Collection date	Accession No				
				ITS	nLSU	*rpb1*	*rpb2*	*tef1a*
Pseudohyphodermella poroides	Dai 12045	China: Hainan	25 Nov 2010	KX008367	KX011852			
Quasiphlebia densa	WEI 17-057	USA: Georgia	23 Apr 2017	MZ637066	MZ637265	MZ748410	OK135986	MZ913630
Quasiphlebia densa	Wu 9304-33	Taiwan	13 Apr 1993	MZ637067	MZ637266	MZ748409		MZ913629
Rhizochaete brunnea	MR11455	Argentina	23 Mar 1998	AY219389	AY219389			
Rhizochaete fouquieriae	KKN121 sp	USA: Arizona		KY948786	KY948858			
Rhizochaete radicata	FD-123	USA: Massachusetts		KP135407	KP135279			
Riopa metamorphosa	JV 0511/5	Czech Republic		KX752613	KX752613			
Riopa pudens	Cui 3238	China	22 Oct 2005	JX623931	JX644060			
Roseograndinia aurantiaca	CLZhao 10487	China: Yunnan	10 Jan 2019	MW209023	MW209012			
Roseograndinia aurantiaca	CLZhao 10491	China: Yunnan	10 Jan 2019	MW209024	MW209013			
Roseograndinia jilinensis	Wu 1307-132	China: Jilin	14 Jul 2013	MZ637076	MZ637274	MZ748412	OK135984	MZ913631
Roseograndinia jilinensis	Wu 1307-137	China: Jilin	14 Jul 2013	MZ637077	MZ637275	MZ748413	OK135985	MZ913632
Roseograndinia minispora	WEI 18-508	China: Taiwan	05 Nov 2018	MZ637078	MZ637276			
Roseograndinia minispora	WEI 18-511	China: Taiwan	05 Nov 2018	MZ637079	MZ637277			
Roseograndinia zixishanensis	CLZhao 7206	China: Yunnan	01 Aug 2018	MZ305280	MZ305289			
Roseograndinia zixishanensis	CLZhao 7718	China: Yunnan	01 Aug 2018	MZ305285	MZ305293			
Scopuloides rimosa	HHB-7042-Sp	USA: Florida		KP135350	KP135282			
Terana caerulea	FP-104073	USA: Maryland		KP134980	KP135276			

Newly generated sequences are in bold

Jun 2019, *Li-Wei Zhou*, LWZ 20190613-54 (HMAS 287394—holotype).

Description: *Basidiomes* annual, resupinate, adnate, adherent, without odor or taste, leathery when fresh, up to 2.5 cm wide, 15 cm long and 100–150 µm thick. Hymenophoral surfaces smooth to tuberculate, shaped with the substrate shape partly, white to pale buff when fresh, becoming darker buff pale and cracking when drying. Margin distinct, white.

Hyphal system monomitic; generative hyphae with simple septa, thin-walled, 2.5–4 µm ($n=40/2$) diam, branched, acyanophilous, inamyloid, indextrinoid, interwoven in subhymenium, more or less regularly arranged in subiculum; tissue unchanged in KOH. *Basidia* clavate, with four sterigmata and a basal simple septum, 20–25 × 5.5–6.5 µm ($n=40/2$); basidioles dominant, in shape similar to basidia, but slightly smaller. *Cystidia* and cystidioles absent; cystidioid hyphal ends occasionally present, narrow clavate, thin-walled. Crystals present among hyphae, rhomboidal. *Basidiospores* ellipsoid, hyaline, thin-walled, smooth, inamyloid, indextrinoid, acyanophilous, (4.1–)4.2–5.2(–5.3) × 3.1–3.9(–4) µm, L = 4.81 µm, W = 3.42 µm, Q = 1.39–1.44 ($n=60/2$).

Additional specimen examined: **Malaysia:** *Kuala Lumpur*: KL Forest Eco park, on fallen angiosperm twig, 8 Dec 2019, *Li-Wei Zhou*, LWZ 20191208-13 (HMAS 287395).

Notes: *Hyphodermella suiae* is similar to *H. brunneocontexta* in the smooth to tuberculate hymenophoral surface and the size of basidiospores. However, the hyphae of *H. brunneocontexta* in subiculum are thick-walled and brown (Duhem and Buyck 2011), while *H. suiae* has thin-walled, hyaline hyphae. In addition, *H. suiae* differs in having smaller basidiospores than the three species of *Hyphodermella* sampled in the current phylogenetic analysis, viz. *H. corrugate* (7–10 × 4–6 µm, Eriksson and Ryvarden 1976), *H. pallidostraminea*

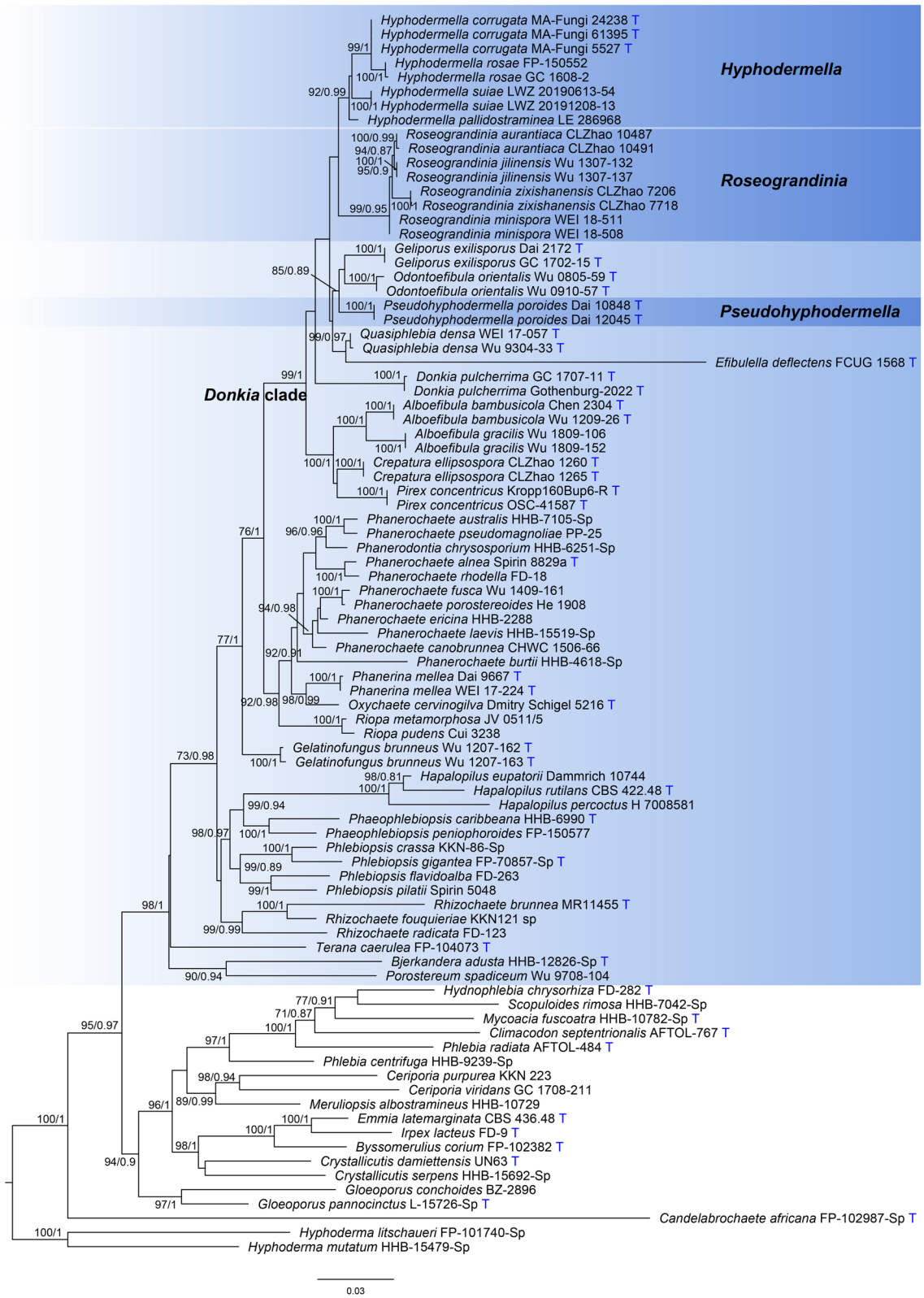

Fig. 2 Phylogenetic relationships among *Hyphodermella* and related genera inferred from ITS and nLSU regions. The topology was generated from the maximum likelihood algorithm, and bootstrap values and Bayesian posterior probabilities simultaneously above 50% and 0.8, respectively, are presented at the nodes. *Phanerochaetaceae* is indicated by the background in blue color, and the three genera related to *Hyphodermella* in darker blue color. The generic type species are indicated by the blue character T at the end of tip labels

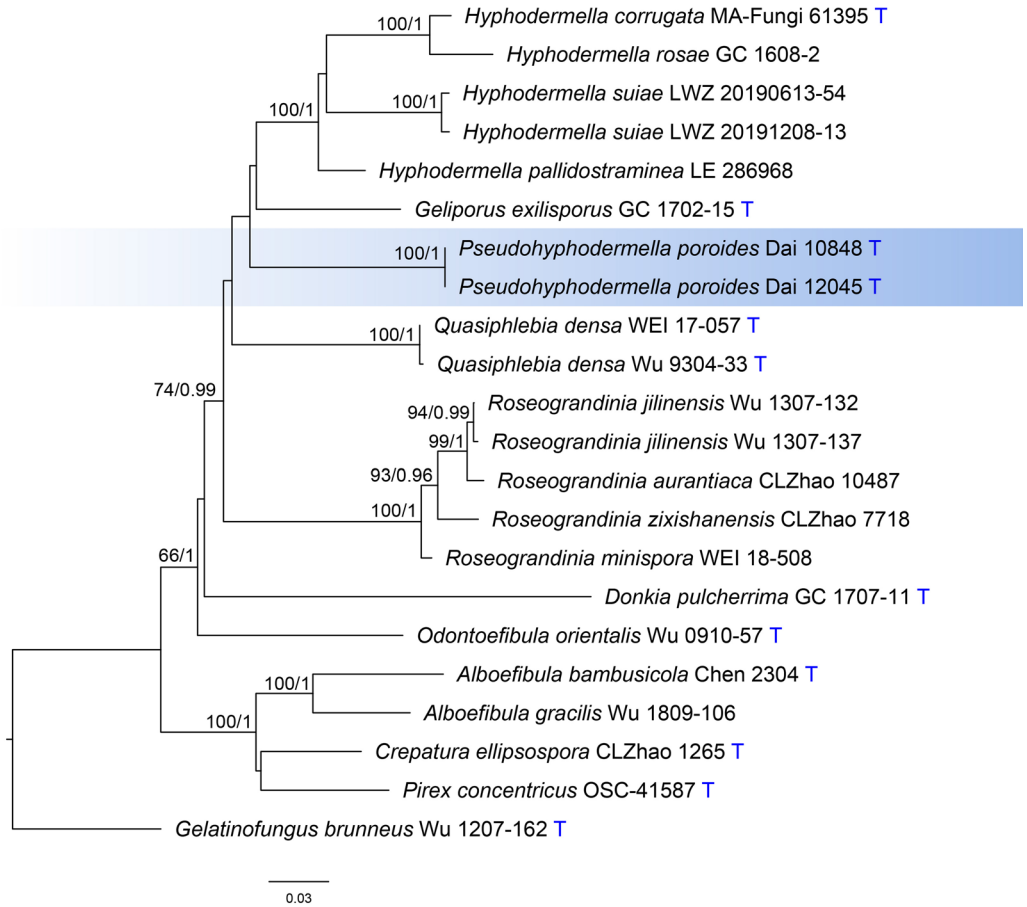

Fig. 3 Phylogenetic relationships among *Hyphodermella* and related genera inferred from ITS, nLSU, *rpb1*, *rpb2* and *tef1a* regions. The topology was generated from the maximum likelihood algorithm, and bootstrap values and Bayesian posterior probabilities simultaneously above 50% and 0.8, respectively, are presented at the nodes. *Pseudohyphodermella* is indicated by the background in blue color. The generic type species are indicated by the blue character T at the end of tip labels

(5.4–6.6×3–3.5 µm, Crous et al. 2021), and *H. rosae* (6–8×4.3–5 µm, Nakasone 2008).

Pseudohyphodermella Shan Shen, S.L. Liu & L.W. Zhou, **gen. nov**.

MycoBank: MB 848651

Etymology: *Pseudohyphodermella* (Lat.), referring to the incorrect placement of the generic type in *Hyphodermella*.

Diagnosis: Distinguished from other genera in *Phanerochaetaceae* by the annual, resupinate basidiomes, a poroid hymenophore configuration, tissues unchanged in KOH, absence of cystidia, and broadly ellipsoid basidiospores.

Type: *Pseudohyphodermella poroides* (Y.C. Dai & C.L. Zhao) Shan Shen et al. 2023.

Description: *Basidiomes* annual, resupinate, effused. Hymenophoral surface poroid, cream to orange. *Hyphal system* monomitic; generative hyphae with simple septa, hyaline, thin-walled, wider in subiculum than in trama. *Cystidia* absent. *Basidia* clavate, hyaline, thin-walled, with four sterigmata and a basal simple septum. *Basidiospores* broadly ellipsoid, hyaline, thin-walled, smooth, inamyloid, indextrinoid, acyanophilous.

Notes: Within the *Donkia* clade of *Phanerochaetaceae*, the poroid hymenophoral surface makes *Pseudohyphodermella* and *Geliporus* distinct from other genera. Moreover, the tissues of *Pseudohyphodermella* do not change in KOH and the basidiospores are broadly ellipsoid (Zhao

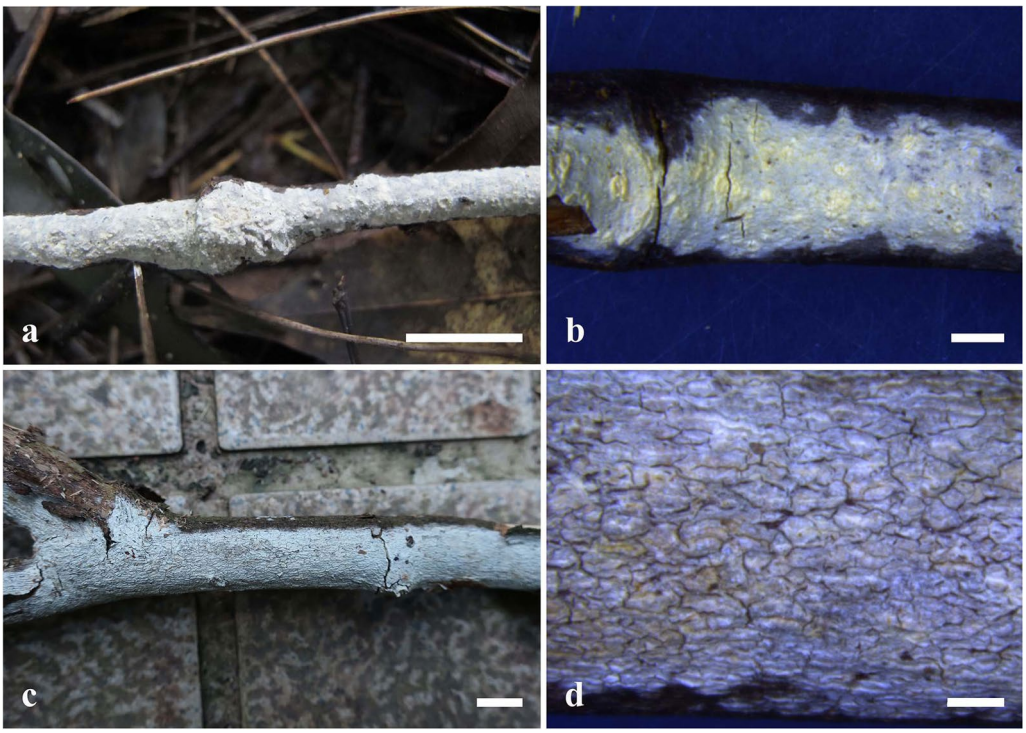

Fig. 4 Basidiomes of *Hyphodermella suiae* (**a**–**d**) in general and detailed views. **a**, **b** LWZ 20190613-54 (holotype); **c**, **d** LWZ 20191208-13 (paratype). Bars: **a**, **c** = 1 cm; **b**, **d** = 2 mm

et al. 2017), while *Geliporus* has tissues that darken in KOH and cylindric to oblong-ellipsoid basidiospores (Yuan et al. 2017). In addition, *Phanerina* and *Riopa* fall outside the *Donkia* clade but within *Phanerochaetaceae* but also resemble *Pseudohyphodermella* in having resupinate basidiomes with a poroid hymenophoral surface; however, these two genera differ in the presence of cystidia and curved cylindrical to narrow ellipsoid basidiospores (Miettinen et al. 2016).

Pseudohyphodermella poroides (Y.C. Dai & C.L. Zhao) Shan Shen, S.L. Liu & L.W. Zhou, **comb. nov.**

MycoBank: MB 848652

Basionym: *Hyphodermella poroides* Y.C. Dai & C.L. Zhao, *Mycoscience* **58**: 454 (2017).

Notes: *Pseudohyphodermella poroides* was originally described in *Hyphodermella* with a simple phylogeny as reference (Zhao et al. 2017). Although this species shares some morphological characters with *Hyphodermella*, such as a monomitic hyphal system with simple-septate generative hyphae and absence of cystidia, its poroid hymenophoral surface makes it distinguished from other species of *Hyphodermella*. Chen et al. (2021) first revealed the separation of *H. poroides* from *Hyphodermella* from a phylogenetic perspective. The current phylogeny (Fig. 2) further confirms the independence of *H. poroides* from all known genera and species. Therefore, a new genus *Pseudohyphodermella* is erected for this species, and *H. poroides* is accordingly transferred as *P. poroides.*

Roseograndinia aurantiaca (C.L. Zhao) Shan Shen, S.L. Liu & L.W. Zhou, **comb. nov.**

MycoBank: MB 848653

Basionym: *Hyphodermella aurantiaca* C.L. Zhao, *Ann. bot. fenn.* **58**: 65 (2020).

Notes: *Hyphodermella aurantiaca* was recently described as a new species; however, the original simple phylogenies inferred from the nLSU region and a combination of ITS and nLSU regions did not provide reliable statistical support for the taxonomic position of this species in *Hyphodermella* (Wang and Zhao 2020). With our more comprehensive sampling, the current phylogeny strongly supports *H. aurantiaca* being separated from *H. corrugata* the type species of *Hyphodermella* and grouping together with species of *Roseograndinia* (BS = 99%, BPP = 0.95; Fig. 2). Morphologically, the combination of rose-colored

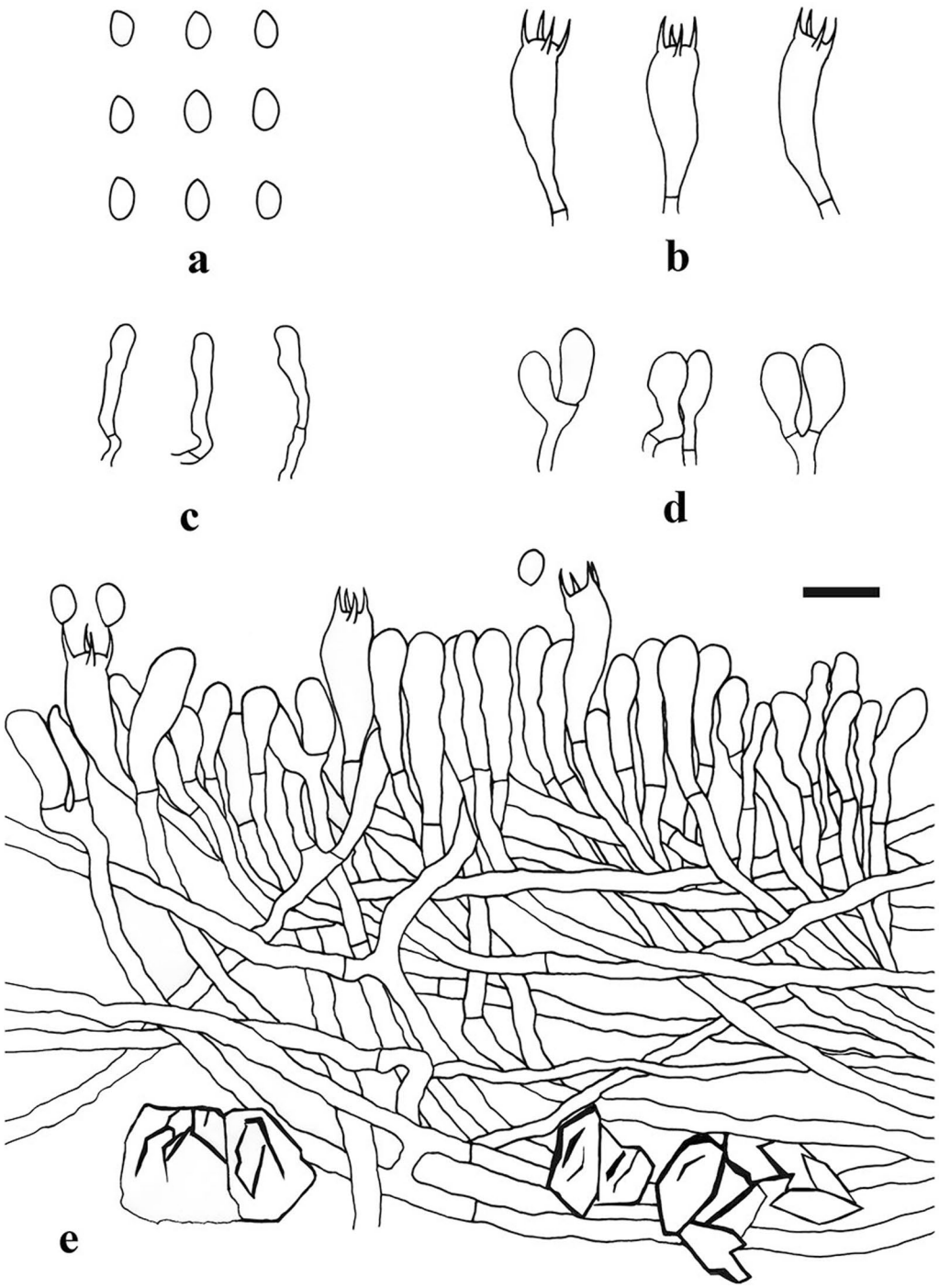

Fig. 5 Microscopic structures of *Hyphodermella suiae* (drawn from LWZ 20190613-54, holotype). **a** Basidiospores. **b** Basidia. **c** Cystidioid hyphal ends. **d** Basidioles. **e** A vertical section through basidiomes. Bars: 10 µm

basidiomes with a smooth to tuberculate hymenophoral surface, absence of cystidia and ellipsoid basidiospores makes *H. aurantiaca* consistent with the concept of *Roseograndinia* sensu Chen et al. (2021). Accordingly, *H. aurantiaca* is transferred as *Roseograndinia aurantiaca*.

Roseograndinia zixishanensis (C.L. Zhao) Shan Shen, S.L. Liu & L.W. Zhou, **comb. nov.**

MycoBank: MB 848654

Basionym: *Hyphodermella zixishanensis* C.L. Zhao, *Nordic Jl Bot.* 38(8): e03329, 4 (2021).

Notes: *Hyphodermella zixishanensis* was described as a new species in *Hyphodermella* (Wang et al. 2021a, b) soon after the publication of *H. aurantiaca* (Wang and Zhao 2020). Like Wang and Zhao (2020), the simple phylogenies in Wang et al. (2021ab) also did not reliably support the taxonomic position of this species in *Hyphodermella*. Instead, *H. zixishanensis* and *H. aurantiaca* formed a strongly supported clade (Wang et al. 2021a, b). The current phylogeny with a more comprehensive sampling strongly supports a close phylogenetic relationship between these two species and *Roseograndinia* (Fig. 2). Morphologically, *H. zixishanensis* is characterized by reddish, ceraceous basidiomes with a tuberculate hymenophoral surface and the absence of cystidia, which fits the concept of *Roseograndinia* sensu Chen et al. (2021). Therefore, *H. zixishanensis* is transferred as *Roseograndinia zixishanensis*.

A key to all eight known species in *Hyphodermella*

1 Basidiospores > 8 µm in length	2
Basidiospores < 8 µm in length	3
2 (1) Hymenophore surface orange to yellow orange; basidia > 35 µm in length	*H. corrugata*
Hymenophore surface ochraceous; basidia < 35 µm in length	*H. ochracea*
3 (1) Cystidia present	*H. maunakeaensis*
Cystidia absent	4
4 (3) Hymenophore surface odontioid	5
Hymenophore surface smooth to tuberculate	6
5 (4) Basidia suburniform to cylindric, 18–25 × 5–6.5 µm	*H. densa*
Basidia more or less clavate, 24–35 × 6–8 µm	*H. rosae*
6 (4) Hyphae thin-walled	*H. suiae*
Hyphae thick-walled, especially in subiculum	7
7 (6) Basidiomes pale yellowish; generative hyphae hyaline	*H. pallidostraminea*
Basidiomes pale grey or olive or brown; generative hyphae brown to dark brown in subiculum	*H. brunneocontexta*

A key to all five known species in *Roseograndinia*

1 Hymenophoral surface grandinioid to odontioid	2
Hymenophoral surface smooth to tuberculate	3
2 (1) Basidiospores < 3.1 µm in width, each with 1–2 oil drops	*R. jilinensis*
Basidiospores > 3.1 µm in width, without oil drops	*R. rosea*
3 (1) Basidia > 20 µm in length	*R. zixishanensis*
Basidia < 20 µm in length	4
4 (3) Basidiomes to 130 µm thick; basidiospores > 4 µm in length	*R. minispora*
Basidiomes 300–500 µm thick; basidiospores < 4 µm in length	*R. aurantiaca*

DISCUSSION

With the most comprehensive sampling to date in the current phylogenetic analyses (Figs. 2, 3), our specimens were identified as definitely belonging in *Hyphodermella*, being described as a new species, *H. suiae*. Although the current two-locus based phylogeny (Fig. 2) and the previous phylogenies related to *Hyphodermella* (Zhao et al. 2017; Wang and Zhao 2020; Chen et al. 2021; Wang et al. 2021a) are all inferred from the ITS and nLSU regions, the relationship at the generic level will be more accurate with sampling more comprehensive taxa in phylogenetic analyses (Fig. 2; Chen et al. 2021: Fig. 3). Furthermore, the five-locus based phylogenetic analysis we performed and the resulting phylogeny (Fig. 3) further confirmed the accuracy of phylogenetic relationships among sampled species of *Hyphodermella* inferred from the ITS and nLSU regions. Accordingly, *Hyphodermella aurantiaca*, *H. poroides* and *H. zixishanensis* are all excluded from *Hyphodermella*.

Hyphodermella poroides, occupying an independent phylogenetic position (Figs. 2, 3), is placed in a newly introduced monotypic genus *Pseudohyphodermella*. This new genus forms a weakly supported clade with *Geliporus* and *Odontoefibula* in the two-locus based phylogeny (BS = 85%, BPP = 0.89; Fig. 2), and has no close relationship with these two genera or any other genera in the five-locus based phylogeny (Fig. 3). Therefore, the alternative options of generic delimitation instead of erecting the new monotypic genus as suggested by Vellinga et al. (2015) cannot be supported according to the current phylogenies.

Roseograndinia was erected as a monotypic genus for *R. rosea* (Hjortstam and Ryvarden 2005). Due to a lack of molecular sequences from the type species of the genus, *R. rosea*, the phylogenetic independence of this genus in *Phanerochaetaceae* was recovered by two morphologically similar species *R. jilinensis* and *R. minispora* (Chen et al. 2021) and we follow the taxonomic proposal by Chen et al. (2021). The current phylogenies (Figs. 2, 3)

strongly support the clade comprising *H. aurantiaca*, *H. zixishanensis*, *R. jilinensis*, and *R. minispora*. Moreover, morphologically *H. aurantiaca* and *H. zixishanensis* also fit well with the concept of *Roseograndinia* sensu Chen et al. (2021). Therefore, *H. aurantiaca* and *H. zixishanensis* are transferred as *R. aurantiaca* and *R. zixishanensis* here.

We note that in the current five-locus based phylogenetic analysis, only ITS and nLSU regions are used for the *Pseudohyphodermella* lineage. That is because additional gene regions were not published when *P. poroides* was originally described (Zhao et al. 2017), and moreover, the type specimens are also unavailable for molecular sequencing as they appear to be missing from the collections of the Institute of Microbiology, Beijing Forestry University, where the types were originally deposited. Even then, according to the separation of *Hyphodermella* and *Roseograndinia* in both the two-locus and five-locus based phylogenies (Figs. 2, 3), and the separation of *Pseudohyphodermella* from *Hyphodermella* and *Roseograndinia* in the two-locus based phylogeny (Fig. 2), it is reasonable to postulate that *Pseudohyphodermella* is a *bona fide* distinct lineage from others. Taking previous phylogenies of *Hyphodermella* (Zhao et al. 2017; Wang and Zhao 2020; Chen et al. 2021; Wang et al. 2021a) into consideration together, our study indicates that the ITS and nLSU regions are enough to delimit generic circumscriptions if the related genera are comprehensively sampled in phylogenetic analyses. Namely, sampling more taxa prior to employing more genes is more crucial to explore phylogenetic relationships among genera, at least those related to *Hyphodermella*. Normally, it is better to sample all known genera in a certain family, but we recognize that sometimes this is quite difficult, if possible, when the targeted genera belong to a phylogenetically not well-resolved family. So, we suggest comprehensively sampling at least closely related genera with targeted genera in taxonomic studies in these fungi.

CONCLUSION

In conclusion, species originally belonging to *Hyphodermella* are placed in three genera, including *Hyphodermella*, a new genus *Pseudohyphodermella*, and *Roseograndinia*, and *H. suiae* is described as a new species. Beyond resolving the taxonomy of *Hyphodermella* itself, this study further clarified that simple phylogenies cannot always accurately place species in appropriate genera. This is an obvious but sometimes omitted phylogenetic practice in recent years (Guan et al. 2020; Zong et al. 2021; Li et al. 2022a; Liu et al. 2022c). We suggest that all fungal taxonomists especially beginners should keep in mind to sample as many comprehensive taxa as possible in phylogenetic, and for that matter morphological analyses (Hawksworth 2020).

Abbreviations

BI	Bayesian inference
BPP	Bayesian posterior probability
BS	Bootstrap
CTAB	Cetyl-trimethyl-ammonium bromide
ML	Maximum likelihood
PCR	Polymerase chain reaction

Supplementary Information

The online version contains supplementary material available at https://doi.org/10.1186/s43008-023-00116-7.

Additional file 1: Alignment S1. The concatenated alignment of ITS and nLSU.

Additional file 2: Alignment S2. The concatenated alignment of ITS, nLSU, *rpb1*, *rpb2* and *tef1a* regions.

Acknowledgements

Dr. Genevieve Gates (Tasmanian Institute of Agriculture, Australia) is thanked for polishing the English language.

Author contributions

SS and S-LL made morphological examinations and performed phylogenetic analyses. L-WZ conceived and supervised the work. SS, S-LL and L-WZ wrote the manuscript. All authors approved the manuscript.

Funding

The research was financed by the National Natural Science Foundation of China (Project Nos. 32100004, 31970012 & 32111530245).

Availability of data and materials

All sequence data generated for this study can be accessed via GenBank: https://www.ncbi.nlm.nih.gov/genbank/.

Declarations

Ethics approval and consent to participate

Not applicable.

Consent for publication

Not applicable.

Competing interests

The authors declare no competing interests.

Received: 14 November 2022 Accepted: 24 May 2023
Published online: 06 June 2023

References

Bengtsson-Palme J, Ryberg M, Hartmann M, Branco S, Wang Z, Godhe A et al (2013) Improved software detection and extraction of ITS1 and ITS2 from ribosomal ITS sequences of fungi and other eukaryotes for analysis of environmental sequencing data. Methods Ecol Evol 4:914–919. https://doi.org/10.1111/2041-210X.12073

Capella-Gutiérrez S, Silla-Martínez JM, Gabaldón T (2009) trimAl: a tool for automated alignment trimming in large-scale phylogenetic analyses. Bioinformatics 25:1972–1973. https://doi.org/10.1093/bioinformatics/btp348

Chen CC, Chen CY, Wu SH (2021) Species diversity, taxonomy and multigene phylogeny of phlebioid clade (*Phanerochaetaceae*, *Irpicaceae*,

Meruliaceae) of *Polyporales*. Fungal Divers 111:337–442. https://doi.org/10.1007/s13225-021-00490-w
Chikowski RS, Larsson KH, Gibertoni TP (2020) Taxonomic novelties in *Trechispora* (*Trechisporales*, *Basidiomycota*) from Brazil. Mycol Prog 19:1403–1414. https://doi.org/10.1007/s11557-020-01635-y
Crous PW, Osieck ER, Jurjevi Ž, Boers J, van Iperen AL, Starink-Willemse M et al (2021) Fungal planet description sheets: 1284–1382. Persoonia 47:178–374
Dai YC, Cui BK, Si J, He SH, Hyde KD, Yuan HS et al (2015) Dynamics of the worldwide number of fungi with emphasis on fungal diversity in China. Mycol Prog 14:62. https://doi.org/10.1007/s11557-015-1084-5
Duhem B (2010) Le genre *Hyphodermella* en France. Bulletin De La Société Mycologique De France 125:137–168
Duhem B, Buyck B (2011) *Hyphodermella brunneocontexta* sp. nov. (*Basidiomycota*, *Polyporales*) de l'île de Mayotte (France). Cryptogamie Mycologia 32:413–420. https://doi.org/10.7872/crym.v32.iss4.2011.413
Eriksson J, Ryvarden L (1976) The Corticiaceae of North Europe. Volume 4. *Hyphodermella—Mycoacia*. Fungiflora, Oslo
Gardes M, Bruns TD (1993) ITS primers with enhanced specifity for basidiomycetes: application to identification of mycorrhizae and rusts. Mol Ecol 2:113–118. https://doi.org/10.1111/j.1365-294x.1993.tb00005.x
Gilbertson RL, Desjardin DE, Rogers JD, Hemmes DE (2001) Fungi from the Mamane-Naio vegetation zone of Hawai'i. Fungal Divers 6:35–69
Guan QX, Liu CM, Zhao TJ, Zhao CL (2020) *Heteroradulum yunnanensis* sp. nov. (*Auriculariales*, *Basidiomycota*) evidenced by morphological characters and phylogenetic analyses in China. Phytotaxa 437:51–59. https://doi.org/10.11646/phytotaxa.437.2.1
Guindon S, Gascuel O (2003) A simple, fast, and accurate algorithm to estimate large phylogenies by maximum likelihood. Syst Biol 52:696–704. https://doi.org/10.1080/10635150390235520
Hawksworth DL, Lücking R (2017) Fungal diversity revisited: 2.2 to 3.8 million species. Microbiol Spectrum 5:FUNK-0052–2016. https://doi.org/10.1128/9781555819583.ch4
Hawksworth DL (2020) Lessons from fifty years describing and classifying fungi. Kavaka 55:1–11. https://doi.org/10.36460/kavaka/55/2020/1-11
Hjortstam K, Ryvarden L (2005) New taxa and new combinations in tropical corticioid fungi (*Basidiomycotina*, *Aphyllophorales*). Synopsis Fungorum 20:33–41
Kalyaanamoorthy S, Minh BQ, Wong TKF, von Haeseler A, Jermiin LS (2017) ModelFinder: fast model selection for accurate phylogenetic estimates. Nat Methods 14:587–589. https://doi.org/10.1038/nmeth.4285
Katoh K, Standley DM (2013) MAFFT multiple sequence alignment software version 7: improvements in performance and usability. Mol Biol Evol 30:772–780. https://doi.org/10.1093/molbev/mst010
Katoh K, Kuma K, Toh H, Miyata T (2005) MAFFT version 5: improvement in accuracy of multiple sequence alignment. Nucleic Acids Res 33:511–518. https://doi.org/10.1093/nar/gki198
Li JJ, Zhao CL, Liu CM (2022a) The morphological characteristics and phylogenetic analyses revealed an additional taxon in *Heteroradulum* (*Auriculariales*). Diversity 14:40. https://doi.org/10.3390/d14010040
Li QZ, Liu SH, Wang XW, May TW, Zhou LW (2022b) Redelimitation of *Heteroradulum* (*Auriculariales*, *Basidiomycota*) with *H. australiense* sp. nov. MycoKeys 86:87–101. https://doi.org/10.3897/mycokeys.86.76425
Liu YJ, Whelen S, Hall BD (1999) Phylogenetic relationships among ascomycetes: evidence from an RNA polymerse II subunit. Mol Biol Evol 16:1799–1808. https://doi.org/10.1093/oxfordjournals.molbev.a026092
Liu SL, He SH, Wang XW, May TW, He G, Chen SL et al (2022a) *Trechisporales* emended with a segregation of *Sistotremastrales* ord. nov. Mycosphere 13:862–954. https://doi.org/10.5943/mycosphere/13/1/11
Liu SL, Shen ZQ, Li QZ, Liu XY, Zhou LW (2022b) *Alloexidiopsis* gen. nov., a revision of generic delimitation in *Auriculariales* (*Basidiomycota*). Front Microbiol 13:894641. https://doi.org/10.3389/fmicb.2022.894641
Liu ZB, Wu YD, Zhao H, Lian YP, Wang YR, Wang CG, et al (2022c) Outline, divergence times, and phylogenetic analyses of *Trechisporales* (*Agaricomycetes*, *Basidiomycota*). Front Microbiol 13:818358. https://doi.org/10.3389/fmicb.2022.818358
Matheny PB (2005) Improving phylogenetic inference of mushrooms with RPB1 and RPB2 nucleotide sequences (Inocybe; Agaricales). Mol Phylogenet Evol 35:1–20
Matheny PB, Liu YJ, Ammirati JF, Hall BD (2002) Using RPB1 sequences to improve phylogenetic inference among mushrooms (*Inocybe*, *Agaricales*). Am J Bot 89:688–698. https://doi.org/10.3732/ajb.89.4.688
Melo I, Hjortstam K (2003) A new species of *Hyphodermella* (basidiomycetes, *Aphyllophorales*) from Portugal. Nova Hedwigia 77:351–355. https://doi.org/10.1127/0029-5035/2003/0077-0351
Miettinen O, Spirin V, Vlasák J, Rivoire B, Stenroos S, Hibbett D (2016) Polypores and genus concepts in *Phanerochaetaceae* (*Polyporales*, *Basidiomycota*). MycoKeys 17:1–46. https://doi.org/10.3897/mycokeys.17.10153
Minh BQ, Schmidt HA, Chernomor O, Schrempf D, Woodhams MD, von Haeseler A et al (2020) IQ-TREE 2: new models and efficient methods for phylogenetic inference in the genomic era. Mol Biol Evol 37:1530–1534. https://doi.org/10.1093/molbev/msaa015
Nakasone KK (2008) Type studies of corticioid hymenomycetes described by Bresadola. Cryptogamie Mycologie 29:231–257. https://doi.org/10.33585/cmy.64104
Niskanen T, Douglas B, Kirk P, Crous P, Lücking R, Matheny PB, et al (2018) New discoveries: Species of fungi described in 2017. In: Willis KJ (ed) State of the World's Fungi 2018. Royal Botanic Gardens, Kew, pp 18–23
Posada D (2008) jModelTest: phylogenetic model averaging. Mol Biol Evol 25:1253–1256. https://doi.org/10.1093/molbev/msn083
Prasanna AN, Gerber D, Kijpornyongpan T, Aime MC, Doyle VP, Nagy LG (2020) Model choice, missing data, taxon sampling impact phylogenetic inference of deep *Basidiomycota* relationships. Syst Biol 69:17–37. https://doi.org/10.1093/sysbio/syz029
Rehner SA, Buckley E (2005) A *Beauveria* phylogeny inferred from nuclear ITS and EF1-α sequences: evidence for cryptic diversification and links to *Cordyceps* teleomorphs. Mycologia 97:84–98. https://doi.org/10.3852/mycologia.97.1.84
Ronquist F, Teslenko M, van der Mark P, Ayres D, Darling A, Höhna S et al (2012) MrBayes 3.2: efficient Bayesian phylogenetic inference and model choice across a large model space. Syst Biol 61:539–542. https://doi.org/10.1093/sysbio/sys029
Telleria MT, Dueñas M, Melo I, Martín MP (2010) Morphological and molecular studies of *Hyphodermella* in the Western Mediterranean area. Mycol Prog 9:585–596. https://doi.org/10.1007/s11557-010-0666-5
Vellinga EC, Kuyper TW, Ammirati J, Desjardin DE, Halling RE, Justo A et al (2015) Six simple guidelines for introducing new genera of fungi. IMA Fungus 6:A65–A68. https://doi.org/10.1007/BF03449356
Wang H, Zhao CL (2020) *Hyphodermella aurantiaca* sp. nova (*Polyporales*, Basidiomycota) as evidenced by morphological characters and phylogenetic analyses. Ann Bot Fenn 58:61–68. https://doi.org/10.5735/085.058.0110
Wang XW, May TW, Liu SL, Zhou LW (2021b) Towards a natural classification of *Hyphodontia* sensu lato and the trait evolution of basidiocarps within *Hymenochaetales* (*Basidiomycota*). J Fungi 7:478. https://doi.org/10.3390/jof7060478
Wang H, Gu ZR, Zhao CL (2021a) *Hyphodermella zixishanensis* (*Polyporales*, *Basidiomycota*), a new species with reddish hymenial surface. Nordic J Bot 39:e03329. https://doi.org/10.1111/njb.03329
White TJ, Bruns T, Lee S, Taylor J (1990) Amplification and direct sequencing of fungal ribosomal RNA genes for phylogenetics. In: PCR Protocols: A guide to methods and applications (eds. Innis MA, Gelfand DH, Sninsky JJ, White TJ). Academic Press, New York, pp 315–322. https://doi.org/10.1016/b978-0-12-372180-8.50042-1
Xu TM, Chen YH, Zhao CL (2019) *Trechispora yunnanensis sp. nov.* (*Hydnodontaceae*, *Basidiomycota*) from China. Phytotaxa 424:253–261. https://doi.org/10.11646/phytotaxa.424.4.5
Yu J, Wang XW, Liu SL, Shen S, Zhou LW (2021) Taxonomy and phylogeny of *Resinicium sensu lato* from Asia-Pacific revealing a new genus and five new species (*Hymenochaetales*, *Basidiomycota*). IMA Fungus 12:19. https://doi.org/10.1186/s43008-021-00071-1
Yuan Y, Chen JJ, He SH (2017) *Geliporus exilisporus* gen. et comb. nov., a xanthochroic polypore in *Phanerochaetaceae* from China. Mycoscience 58:197–203. https://doi.org/10.1016/j.myc.2017.01.006
Zhao CL, Ren GJ, Wu F (2017) A new species of *Hyphodermella* (*Polyporales*, *Basidiomycota*) with a poroid hymenophore. Mycoscience 58:452–456. https://doi.org/10.1016/j.myc.2017.06.007

Zong TK, Liu CM, Wu JR, Zhao CL (2021) *Trechispora daweishanensis* and *T. xantha* spp. nov. (*Hydnodontaceae*, *Trechisporales*) found in Yunnan Province of China. Phytotaxa 479:147–159. https://doi.org/10.11646/phytotaxa.479.2.1

Zwickl DJ, Hillis DM (2002) Increased taxon sampling greatly reduces phylogenetic error. Syst Biol 51:588–598. https://doi.org/10.1080/10635150290102339

Publisher's Note